



## Analysis of Radio Frequency Interference Signatures in UAVSAR Polarimetric Data

Mingliang Tao<sup>(1)</sup>, Feng Zhou<sup>(2)</sup>

(1) School of Electronics and Information, Northwestern Polytechnical University, 710072 Xi'an, China

(2) National Laboratory of Radar Signal Processing, Xidian University, 710071 Xi'an, China

### Abstract

Radio frequency interference (RFI) is a critical issue for Polarimetric synthetic aperture radar (PolSAR). The analysis of RFI signatures and its influence on PolSAR data seems to be lacking in existing literatures, especially for PolSAR post products, such as the polarimetric decomposition parameters and clustering result. The goal of this paper is trying to reveal the link between RFI and polarization, as well as to analyze the impact of interference on PolSAR image and post products. Qualitative and quantitative analyses of the adverse impacts of RFI on NASA/JPL UAVSAR dataset are illustrated from two perspectives, i.e., evaluation of imaging quality and interpretation of scattering mechanisms.

### 1. Introduction

It is common to find polarimetric synthetic aperture radar (PolSAR) systems are affected by the radio frequency interference (RFI), especially in low-frequency band [1]. The RFI may come from external electromagnetic devices which share overlapping spectrum with the PolSAR systems, i.e., radiolocation radars, telecommunication devices, television networks, etc. The existences of RFI pose a hindrance to PolSAR image formation and image interpretation [2]. Freeman analyzed the effects of noise on polarimetric SAR data while without discussing the interference [3]. C. Musgrove et al. [4] discusses the impact of interference on coherence and performance of coherent change detection, and some researchers discussed the effect of interference on interferometric phase [5]-[6].

Polarization is the inherent property of electromagnetic wave, and RFI signature is linked to the polarization of the receive channel, depending on the transmission characteristics of the RFI emitter. However, existing literatures seem lacking the analysis of RFI signatures and its influence in PolSAR data, especially for PolSAR post products, such as the polarimetric decomposition parameters and clustering result.

### 2. Distortion Analysis

For a specific polarization channel, the radar echoes could be expressed as a mixture of target echoes, interference from the RFI emitter and system noise,

$$D_{qp}(\hat{t}, t_m) = X_{qp}(\hat{t}, t_m) + I_{qp}(\hat{t}, t_m) + N_{qp}(\hat{t}, t_m) \quad (1)$$

where  $N_{qp}(\hat{t}, t_m)$  denotes the system additive noise.

### 2.1 Influences on Image Quality

In terms of the PolSAR raw data, the direct adverse impact of RFI is the reduction of signal-to-interference-plus-noise power ratio, especially with the presence of strong interference. Very strong RFI emissions could even saturate the receiver. It is not easy to identify the RFI in the time domain because of its additive nature with target echoes. However, RFI may appear well distinguishable in the range-frequency domain because of its relative narrow bandwidth compared to that of the radar echoes.

In case of motion compensation for high-quality SAR image formation, if some critical Doppler parameters (e.g., centroid and modulation rate) need to be estimated from the data, the presence of RFI would yield biased and inaccurate estimates, which would result in blurry and defocusing image or ghosts in the image.

The image formation process could be considered as a process of two-dimensional convolution of the raw echoes with a matched filter kernel in both range and azimuth direction, and expressed as

$$\begin{aligned} \sigma_{qp}(\hat{t}, t_m) &= D_{qp}(\hat{t}, t_m) \oplus G(\hat{t}, t_m) \\ &= X_{qp}^G(\hat{t}, t_m) + I_{qp}^G(\hat{t}, t_m) + N_{qp}^G(\hat{t}, t_m) \end{aligned} \quad (2)$$

where  $\sigma_{qp}$  denotes the imaging result,  $G(\hat{t}, t_m)$  is the system response function of SAR imaging algorithm.  $\oplus$  denotes the two-dimensional convolution operator.

$X_{qp}^G(\hat{t}, t_m)$  is equivalent to the imaging result of useful target echoes, which reflects the reflectivity.  $I_{qp}^G(\hat{t}, t_m)$  and  $N_{qp}^G(\hat{t}, t_m)$  denotes the output of RFI and noise after processing by the image formation step. According to (2), it is shown that the RFI is still mixed with the target echoes in a linear additive nature.

Owning to the 2-D matched filtering processing, PolSAR possesses a large signal processing gain along the range and azimuth, which endows it the inherent capability for interference suppression. It is worth noting that the matched filter is adapted to the target response and not to the RFI and noise. Large-power RFI will still superimpose

on the focused image as visible artifacts or stripes, which may bury the target of interest and cause image quality degradation. For RFI with weak power, it may not be obvious in the amplitude distortion, but may still have strong influence in phase distortion. Incorrect phase would lead to miscalculation of decomposition parameters, and inaccurate interpretation of scattering mechanisms. These will be discussed in next section.

## 2.2 Influences on Interpretation of Scattering Mechanisms

### 1) Polarization Signatures

The ultimate goal of PolSAR imaging is to obtain good understanding and interpretation of the illuminated area. Land-use classification is one of the most important applications of PolSAR. A kind of classification methods is based on the recognition of scattering mechanism between the electromagnetic waves and the medium. The co-polarization and cross-polarization signatures are useful tools for establishing the link with canonical scattering mechanisms.

Knowing the target response in a certain polarization basis, one can synthesize the radar cross section for any arbitrary combination of transmit and receive polarizations with a simple mathematical transformation. Hence, the synthesized 3-D co-polarized signature and cross-polarized signature are expressed as

$$P_{CO} = \left| \left( \mathbf{U} h_p^{rec} \right)^T \cdot \boldsymbol{\sigma} \cdot \left( \mathbf{U} h_p^{tr} \right) \right|^2 = \left| \left( \mathbf{U} h_p^{rec} \right)^T \cdot \left( \mathbf{X}^G + \mathbf{I}^G + \mathbf{N}^G \right) \cdot \left( \mathbf{U} h_p^{tr} \right) \right|^2 \quad (3)$$

$$P_X = \left| \left( \mathbf{U} h_q^{rec} \right)^T \cdot \boldsymbol{\sigma} \cdot \left( \mathbf{U} h_p^{tr} \right) \right|^2 = \left| \left( \mathbf{U} h_q^{rec} \right)^T \cdot \left( \mathbf{X}^G + \mathbf{I}^G + \mathbf{N}^G \right) \cdot \left( \mathbf{U} h_p^{tr} \right) \right|^2 \quad (4)$$

where  $\mathbf{U}$  is the unitary transformation matrix defined by the tilt angle and ellipticity angle of the polarization ellipse characterizing the polarization state.

From (3)-(4), it is shown that the presence of interference would alter the shape and intensity of polarization signatures. Incorrect polarization signature may lead to misunderstanding of the scattering mechanisms, which would result in wrong classification results. Besides, it will also cause error when using the polarization signatures to seek for the optimal polarization combinations. To quantitatively evaluate the influence of interference, two metrics are introduced to compare the similarity between the polarization signatures without RFI and that with RFI, i.e., the normalized signature correlation mapper (NSCM) measures the dissimilarity of the signature shapes, and the Euclidean Distance (ED) used to compare the difference between the intensity of signatures.

### 2) Polarimetric Decompositions

The polarimetric target decomposition theorems aimed at providing interpretation of scattering mechanisms based on sensible physical constrains. The target decomposition

theorems are considered as appropriate tools to perform data interpretation of the distributed targets and have been proved effective for physics-based PolSAR image classification. One of the target decomposition theorems is based on the Eigen decomposition of the covariance matrix or coherence matrix, and then the eigenvalues and eigenvectors are analyzed physically. Among them, the Cloude and Pottier decomposition is a typical representative and we would use it as an example to study the effect of interference on the polarimetric decompositions.

Cloude and Pottier defined the secondary parameters of the Eigen-decomposition, i.e., entropy  $H$ , anisotropy  $A$  and alpha angle  $\bar{\alpha}$ , to describe the randomness in scattering. Correct estimation of  $H/A/\bar{\alpha}$  parameters allow a physical interpretation of PolSAR data. However, the presence of RFI deteriorates the accuracy of Eigen-decomposition, and thus would bias the calculation of these three eigenvalue-derived parameters. C. L. Martinez *et al.* [8] provided thorough perturbation analysis of the eigen-decomposition. It is shown that the biases of the entropy and anisotropy depend only on the eigenvalues, whereas the alpha angle relies also on the eigenvalues and eigenvectors. The biases of eigenvalues and eigenvectors behave as a source of error, and shall be transmitted to the physical parameters obtained from them. Further discussions will be covered in Section 3 by presenting the results of real measured dataset.

## 3. Experimental Results

This dataset is acquired over Hawaii by NASA/JPL UAVSAR in 2010. The illuminated area is a peninsula surrounded by the Pacific Ocean, including an airport, forest, and buildings, etc.

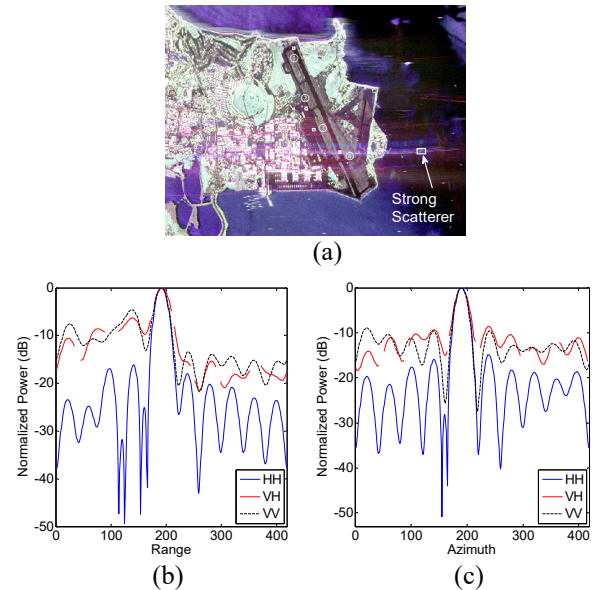


**Figure 1.** UAVAR Hawaii dataset. (a) Pauli-coded image. Sectional drawings of the strong point scatterer along (b) range and (c) azimuth.

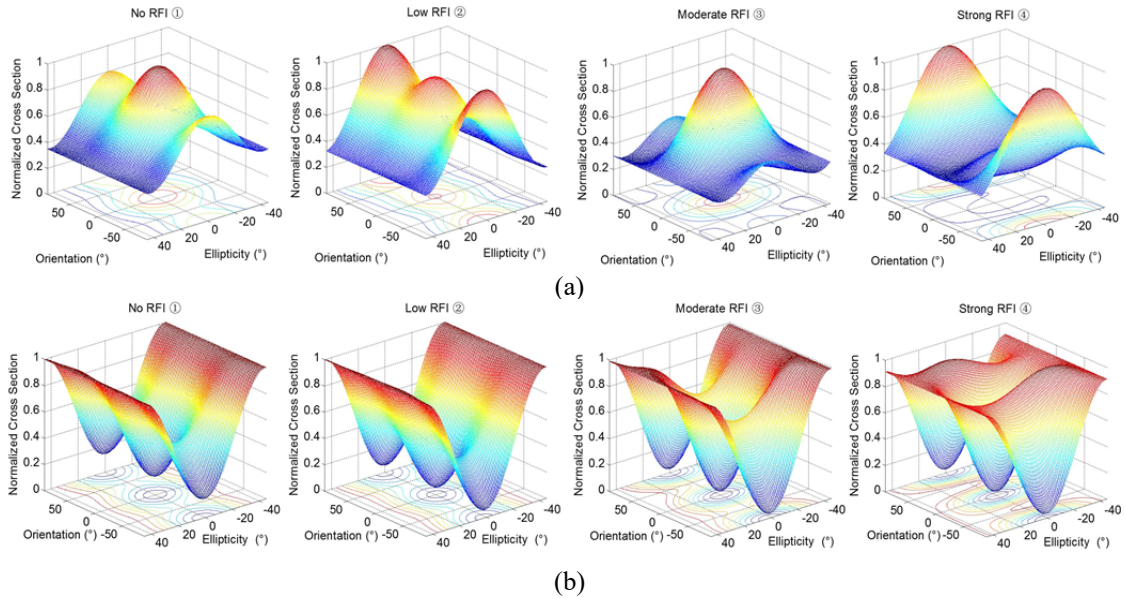


**Figure 2.** Evaluation of the distortion to the polarization signatures under various RFI conditions. (a) NSCM. (b) ED.

Fig. 1(a) presents the image of UAVSAR Hawaii dataset. Obvious RFI stripes are observed and the patterns of the artifacts are very unique, which are not a duplicate of nearby scatterers or areas with strong reflectivity. The patterns are not comparable with the general radiometric artifacts appeared in SAR images such as the ambiguities, saturation effects or processing effects. The patterns in the image are bright stripes with curvature, which could be a result of unmatched filtering of the interference. The interference in this dataset may originate from the nearby airport surveillance radar.

### 3.1 Influence on Image Quality

Since there is no ideal corner reflector in this image for evaluating the point target impulse response, a strong scatterer is extracted out for illustration, as shown in Fig. 1(a). This strong scatterer is a ship target in the sea. Fig.1(b)-(c) plot the sectional drawings of the strong point scatterer along range and azimuth in different polarimetric channels respectively. The transmitting polarization of RFI source is close to vertical polarization, and thus the RFI power in horizontal-receive channel HH is much weaker. However, the presence of interference raises the side-lobe level greatly in VH and VV. The degradation of PSLR and ISLR would make the weak targets easily be submerged, making it difficult to realize target detection.

### 3.2 Influences on Interpretation of Scattering Mechanism

Next, select four areas inside the airport runway corresponding to various RFI conditions for illustration, as marked in Fig. 1(a). They are referred to as *No RFI Area ①*, *Low RFI Area ②*, *Moderate RFI Area ③*, and *Strong RFI Area ④*, respectively. These areas possess the same scattering mechanisms and should have similar reflectivity.

According to (3) and (4), the co-polarized and cross-polarized signatures are computed, as shown in Fig. 2(a)-(b). In *Low RFI Area ②*, the RFI introduces large distortion to the co-polarized signature, while the cross-polarized signature being almost unaffected. Meanwhile, the RFI in *Moderate RFI Area ③* and *Strong RFI Area ④* have a great distortion to the shape and intensity of both the co-polarized and cross-polarized signatures. These four distributed areas should have the same scattering mechanism with the one under ideal occasion, i.e. low ISR condition. Take *No RFI Area ①* as a benchmark, Fig. 3 plots the NSCM and ED values to show the relative deviations of the distorted signatures. The large NSCM and ED values indicate the great changes in shapes and the intensity of signatures. Therefore, the distortion of the image amplitude and phase caused by RFI would lead to erroneous polarization signatures. The erroneous polarization signatures would further bias the interpretation of scattering mechanisms.

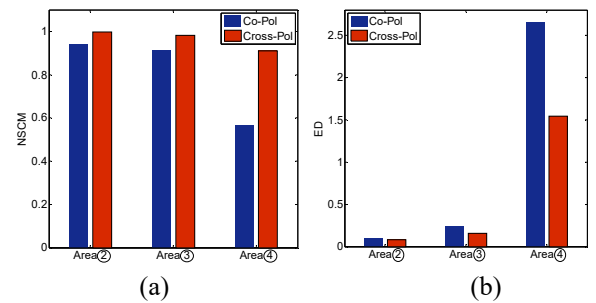


**Figure 3.** Evaluation of the distortion to the polarization signature of marked areas with various RFI conditions. (a) NSCM. (b) ED

A category of land cover classification scheme is based on the physical scattering characteristics. The presence of RFI would derive biased estimate of decomposition parameters, and subsequently lead to wrong classification results when using these incorrect parameters. Next, we take the Cloude-Pottier decomposition as an example to illustrate the effect of interference on target decomposition and classification results. Fig. 4(a)-(c)

shows the  $H/A/\bar{\alpha}$  parameters. From Fig. 4(a)-(b), it is shown that there are many anomalies due to the presence of RFI, especially the sea surface, airport runway, as marked by dashed line. The anomalies clearly show the patterns of interference artifacts. RFI has little effect on the calculation of alpha parameter in Fig. 4(c). This is because the eigenvectors are more robust than the eigenvalues to the presence of RFI. Fig. 4(d) shows the clustering result incorporating the Cloude-Pottier decomposition and the Wishart classifier. It is shown that some areas with and without RFI are misclassified as different classes, such as the airport runway and the nearby sea. The quality of the PolSAR data is negatively affected due to the presence of RFI, with biased retrieval parameters leading to incorrect clustering result.

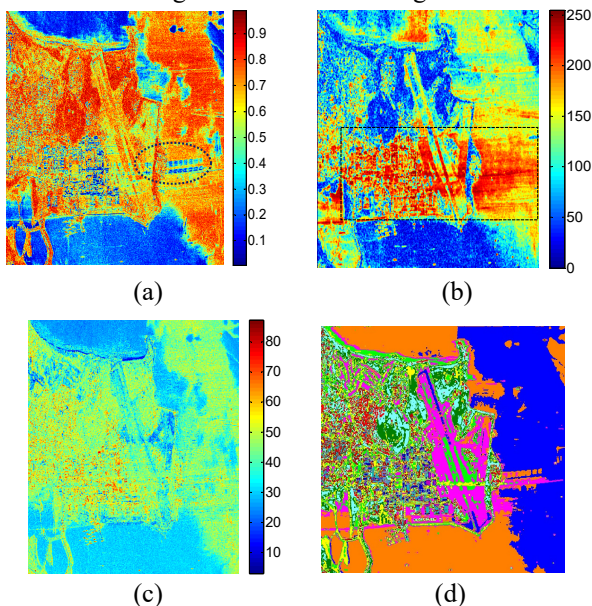


**Figure 4.** Parameters of Cloud-Pottier decomposition, (a) Entropy, (b) Anisotropy, (c) Alpha and (d) clustering result using Wishart Classifier.

## 4 Conclusion

This paper mainly focuses on analyzing the effect of RFI on PolSAR image and post products, without discussing specific interference mitigation methods. Qualitative and quantitative analyses of the adverse impact of RFI on UAVSAR dataset are illustrated from two perspectives, i.e., evaluation of imaging quality and interpretation of scattering mechanisms. The presence of RFI would distort the image amplitude and phase. The noise floor of the image rises with the increase of ISR, which would submerge the image response of weak target, making it difficult to be detected. The resulting distortion to the shape and intensity of both the co-polarized and cross-polarized signatures would lead to misinterpretation of the scattering mechanisms. Moreover, the existence of RFI would induce biased estimation of target decomposition parameter, and thus inaccurate parameters would lead to incorrect clustering result.

## 5. Acknowledgements

This work is supported by Postdoctoral Innovation Talent Support Program under grant BX201700199. This work was supported in part by the National Natural Science Foundation of China under Grant U1430123, 61201283, 61471284 and 61522114, 61601372 and 61601373; it was also supported by the Foundation for the Author of National Excellent Doctoral Dissertation of PR China under Grant 201448, and by the Young Scientist Award of Shaanxi Province under Grants 2015KJXX-19 and 2016KJXX-82. Thanks NASA/JPL for providing the UAVSAR dataset for free downloading.

## 6. References

1. S. Misra, and P. Matthaieis, "Passive remote sensing and radio frequency interference (RFI): an overview of spectrum allocations and RFI management algorithms," *IEEE Geosci. Remote Sens. Mag.*, **2**, 2, June 2014, pp: 68-73, doi: 10.1109/MGRS.2014.2320879.
2. National Academies of Sciences, Engineering, and Medicine. *A Strategy for Active Remote Sensing Amid Increased Demand for Radio Spectrum*. Washington, DC: National Academies Press, 2015. doi: 10.17226/21729.
3. A. Freeman, "The effects of noise on polarimetric SAR data," in *Proc. IEEE Int. Geosci. Remote Sens. Symp.*, **2**, August 1993, pp. 799-802, doi: 10.1109/IGARSS.1993.322215.
4. C. Musgrove, and J. C. West, "Application of equalization notch to improve synthetic aperture radar coherent data products," in *Proc. of SPIE Defense, Security, and Sensing*, Baltimore, Maryland, USA, Apr. 2015, pp. 1-13, doi: 10.1117/12.2175587.
5. M. Pinheiro, M. R. Cassola, P. P. Iraola, A. Reigber, G Krieger, and A. Moreira, "Reconstruction of coherent pairs of synthetic aperture radar data acquired in interrupted mode", *IEEE Trans. Geosci. Remote Sens.*, **52**, 4, April 2015, pp. 1876-1893, doi: 10.1109/TGRS.2014.2350255.
6. H. Xu, Z. Wu, W. Liu, J. Li, and Q. Feng, "Analysis of the effect of interference on InSAR," *IEEE Sensors Journal*, **15**, 10, Oct 2015, pp. 5959-5668, doi: 10.1109/JSEN.2015.2445931.
7. M. Jafari, Y. Maghsoudi, and M. J. Valadan Zoej, "A new method for land cover characterization and classification of polarimetric SAR data using polarimetric signatures," *IEEE J. Sel. Topics Appl. Earth Observ. Remote Sens.*, **8**, 7, July 2015, pp. 3595-3607, doi: 10.1109/JSTARS.2014.2387374.
8. C. L. Martínez, A. A. González, and X. Fàbregas, "Perturbation analysis of eigenvector-based target decomposition theorems in radar polarimetry," *IEEE Trans. Geosci. Remote Sens.*, **52**, 4, Apr 2014, pp. 2081-2095, doi: 10.1109/TGRS.2013.2257802.